RSC Advances

ROYAL SOCIETY OF CHEMISTRY

www.rsc.org/advances

Journal Name

ARTICLE

Adsorption studies of Malachite Green on 5-Sulphosalicylic acid Doped Tetraethoxysilane (SATEOS) Composite Material

Received 00th January 20xx,
Accepted 00th January 20xx

DOI: 10.1039/x0xx00000x

www.rsc.org/

*Sozia Ahad[a], Nasarul Islam[a], Arshid Bashir[a], Suhail-ul Rehman[a] and Altaf Hussain Pandith[a]**

We report batch adsorption studies for the removal of Malachite Green from aqueous solution using 5-sulphosalicylic acid doped tetraethoxysilane (SATEOS) composite material, prepared in our lab earlier. Various variables studied were initial dye concentration, adsorbent concentration, pH, contact time and temperature. Maximum percentage of colour was removed at the basic pH of 9. The removal data were fitted on Langmuir and Freundlich adsorption isotherm equations. The values of their corresponding constants were determined from the slope and intercepts of their respective plots. The monolayer adsorption capacity of SATEOS at 323K was found to be 657.89 mg/g. The values of various thermodynamic parameters like ΔG°, ΔS° and ΔH° were also determined. Pseudo second order kinetic model and Lagergren first order kinetic model were also applied to study adsorption process. The effective diffusion parameter, Di values were estimated at different initial dye concentrations. Mechanism of adsorption was studied using Rechienberg's equation where linearity test indicates film diffusion controlled adsorption mechanism. The maximum interaction (IE =1432.54 KJ (mole)$^{-1}$) between SATEOS and dye molecule, calculated using B3PW91 functional and LanL2MB basis set, was observed when the nitrogen atom of dye lies at a distance of 1.57Å from the hydrogen of hydroxyl group present on SATEOS molecule.

1. Introduction

The effluents from textile, leather, food processing, cosmetic, paper and dye manufacturing industries are important sources of dye pollution. Many dyes and their breakdown products are toxic for living organisms. It is estimated that 10-15% of the dyes have been wasted during the dyeing processes and are directly discharged into water bodies.[1] The dye effluents from various sources not only affect the aesthetic aspects of water bodies but can cause problems in several ways: some of them includes reduction in light penetration, retardation in photosynthetic activity, they can also induce micro-toxicity to fish and other organisms as these dyes have a tendency to chelate with metal ions.[2] It is usually difficult to remove the dyes from water bodies, because mostly dyes are not easily degradable and are generally not removed from waste water by conventional waste water treatments. A vast number of techniques of dye removal have been reported in the literature, which include photodegradation, flocculation, chemical and biological oxidation, ozonation, aerobic and anaerobic microbial degradation, chemical precipitation, ion exchange, filtration,membrane processes[3,4] and adsorption.[5]

In recent years, adsorption technology was extensively used, as adsorption techniques have high potential and can be used as an effective, efficient, and alternative process for the treatment of dye containing wastewater.[6] Owing to its low initial cost, simplicity of design, ease of operation, insensitivity to toxic substances, complete removal of pollutants even from dilute solutions and ability to remove different types of colouring materials, adsorption techniques have received much attention and consideration throughout the world.[7] Removal capacity, treatment cost and operating conditions are important parameters upon which selection of appropriate adsorbents are based.[8] Silica gel,[9] activated alumina,[10] and polymeric porous materials[11] are some of the adsorbents which have been developed and even made commercially available for this purpose. Biopolymer like chitosan is a good adsorbent, used for the removal of various kinds of anionic and cationic dyes as well as heavy metal ions even at lower concentrations.[12] Various kinds of substances have been used to form composite with chitosan such as bentonite, montmorillonite and activated clay.

The improved properties of nanocrystalline materials for adsorption and intra crystalline diffusion afford many potential opportunities for their application in environmental remediation. For example, fullerene and graphene are the two promising functional materials with improved efficiencies for environmental waste cleanup applications. Graphene nanosheets are excellent candidates for adsorption technologies because of their large theoretical specific surface area (2630 m^2g^{-1}). Graphene nanosheets decorated with nanoparticles have been used as novel adsorbents for the removal of contaminants from aqueous solutions.[13] Carbon nanotubes (CNTs) and their composites are also used for the removal of toxic pollutants from waste water and particularly show high efficiencies in removal of organic pollutants from contaminated water.[14] Alginate beads containing magnetic nanoparticles and activated carbon have been used to remove hazardous dyes particularly methylene blue and methyl orange. Similarly, chitosan/montmorillonite nanocomposites have been

*S. Ahad, N. Islam, A. Bashir, S. Rehman and A. H. Pandith**
Department of Chemistry, University of Kashmir
Srinagar-190006 India
Phone: +91-194-2424900(OFFICE), +91-9906424293 (Mobile)
+91-194-2421357
E-mail: altafpandit23@gmail.com,

used to study adsorption characteristic of congo red.[16] It is observed that the nanocomposite have good flocculation ability in aqueous solution, with comparatively low cost and relatively high adsorption capacity.

Malachite Green (MG) has a number of applications ranging from fungicide to disinfectant. It is also used to colour cotton, jute, silk, wool, leather all over the world.[17] Due to its nitrogen composition, MG exhibits carcinogenic, genotoxic, mutagenic, and teratogenic properties. MG is not environmental friendly as it damages the aquatic life by causing detrimental effects in liver, gall bladder, kidney, intestine, and pituitary gonadotrophic cells. Upon inhalation it may cause irritation to the respiratory tract and may also cause irritation to the gastrointestinal tract upon ingestion. It is highly cytotoxic to mammalian cells and acts as a tumor promoting agent.[18,19] From the literature review ,it is found that low cost adsorbents (LCA_S,) have wide availability, fast kinetics and appreciable adsorption capacities.[20] Natural materials which are used as LCA_S, include wood, coal, Peat etc. Various non-conventional sorbents have been specifically reported for their potential to remove MG from aqueous solutions ; some of them are hen feathers,[21] neem leaf powder,[22] modified rice husk,[23] lemon peel,[24] sawdust,[25] tamarind fruit shell,[26] degreased coffee beans,[27] ginger waste,[28] and carbon based adsorbents.[29] Various low cost adsorbent materials including activated carbon,[30,31] neem sawdust,[32] clayey soil,[33] and mango seed husks[34] have also been successfully used for the removal of MG from waste waters.

In this paper, we report batch adsorption studies for the removal of Malachite Green from aqueous solution using 5-sulphosalicylic acid doped tetraethoxysilane (SATEOS) composite material. This material has been synthesized in our lab as reported earlier.[35] We find that the material is highly selective for MG adsorption and, therefore, may have potential applications in the recovery and removal of MG from aqueous media. The adsorption properties of SATEOS composite material was explored as a function of batch operating conditions including, initial solution pH, initial dye concentration, adsorbent concentration, contact time and temperature. Kinetic analysis of the adsorption process was performed in terms of Lagergren first-order and pseudo-second-order kinetic models while as isotherm analysis was carried out in terms of Freundlich and Langmuir isotherm models. Mechanism of adsorption was studied using Rechienberg's equation using linearity test of Bt vs time plots. To understand the nature of the adsorption, thermodynamic parameters were also evaluated. Finally to study the surface morphology of the adsorbent loaded with MG, scanning electron microscopy (SEM) analysis was performed using scanning electron microscope (Model Hitchi-S 3000H) at 20 kV.

2. Experimental

2.1 Materials and instrumentation

The adsorbent material used for this study was SATEOS prepared as reported earlier.[35] The main reagents used for the synthesis of the composite material were tetraethoxysilane (Merck Germany), hexadecyltrimethylammonium chloride (Merck Germany), sulphosalicylic acid (Glaxo Laboratories India Ltd.) and ethyl alcohol. All the starting reagents were of A. R. grade and were used as purchased. The basic dye, Malachite Green having chemical formula $C_{23}H_{25}N_2Cl$, molecular weight 364.63g/mol, was supplied from Ranbaxy laboratories and used as such. Stock solutions of the desired concentration were prepared in double distilled water. The various doses of the SATEOS composite material are mixed with the dye solutions and the mixture was agitated in a mechanical shaker. Keeping all other factors constant, adsorption capacities for different doses were determined at definite time intervals. Characterization of 5-sulphosalicylic acid doped tetraethoxysilane composite material was carried out by the techniques as reported earlier,[31] which involved Fourier transform infrared (FTIR) spectroscopy for measuring IR spectrum of the prepared SATEOS composite material, SEM for taking microphotographs of the original form of the composite material, before and after dye adsoption. The disc techniques using KBr as a matrix was adopted for recording of the spectra and finally X-ray powder diffraction patterns were obtained using diffractometer (Bruker AXS D8 Advance) at 40 kV and 40 mA with Ni-filtered Cu-Kα radiation of wavelength (λ=1.54056 A°).

2.2 Adsorption studies

Batch adsorption experiments were carried out by taking standard dye solutions of known concentrations (30mL) and different adsorbent doses (0.20-1.00g) in 100mL Erlenmeyer flasks, and were agitated in a mechanical shaker to achieve equilibrium. The initial pH of MG solution was measured by pH meter (Thermo Electron Corporation, USA) which was controlled by using 0.1 N hydrochloric acid and 0.1 N sodium hydroxide. To study the effect of solution pH on rate of adsorption of MG, pre weighed amount of SATEOS composite material was added to dye solution (30mL, 5mg/L) at room temperature in the pH range of 1-9 for isothermal shaking at 120 rpm to achieve equilibrium. The amount of adsorbed MG per gram of SATEOS composite material at equilibrium (q_e) was calculated using the following equation:

$$q_e = (C_0 - C_e)\frac{V}{W} \qquad (1)$$

C_0 and C_e are concentrations (mg/L) of MG dye at initial and equilibrium, respectively, V is the volume (L) of the solution and W is the weight (g) of the adsorbent used. The mixture of the Erlenmeyer flasks was filtered after the process reach equilibrium. The concentration of MG in the filtrate was determined using UV-VIS spectrophotometer (Schimadzu UV 3600) at optimum wavelength of 617 nm. Adsorption isotherm studies were carried out by shaking different MG solutions (5-20 mg/L) with a particular adsorbent dose (0.2g) at temperatures 30, 40 and 50°C till equilibrium was observed. The kinetic experiments were carried out by analyzing adsorptive behavior of SATEOS composite material towards MG dye of known concentrations at different time intervals (30-240 min). The effect of contact time was examined using 30 mL of MG solution in the concentration range (5, 10, 15 mg/L) by agitating solution in a mechanical shaker at room temperature containing 0.2g of SATEOS dose. For analyzing the residual dye concentration in the solution, samples were collected from the flasks at predetermined time intervals. After centrifugation the supernatant was analyzed using UV-Visible spectrophotometer (Schimadzu UV 3600) for its residual dye concentration. The amount of dye adsorbed per unit of SATEOS composite material (q_t) at time t was calculated using the following equation:

$$q_t = (C_0 - C_t)\frac{V}{W} \qquad (2)$$

where C_0 and C_t (mg/L) are the concentrations of MG dye at initial and at any time t, respectively. V (L) is the volume of solution and W (g) represents the weight of the SATEOS composite material used.

2.3 Computational studies

All theoretical calculations were carried out using density functional theory (DFT) as incorporated in Gaussian 03 set of codes.[36] Geometry optimizations were performed on isolated entities in

gaseous phase, employing Becke's 3 Perdew Wang 91 (B3PW91)[37] exchange-correlation functional and LanL2MB basis set.[38] Structures of SATEOS, dye and SATEOS-dye combination completely optimized with the subsequent vibrational analysis, corresponded to a minimum on a potential energy surface (PES). To obtain the real time spectral frequencies, all the calculated frequencies were uniformly scaled by 0.97 for all the model compounds.

3. Results and discussions

3.1 Characterization

SEM was used to characterize the surface morphology of SATEOS. It is useful for determining the porosity and appropriate size distribution of the adsorbent. For recording SEM images SATEOS was first stocked over a holder and subsequently gold sputtered before examination. Images were recorded at 5.00 kV with 300V collector bias using Hitchi-S 3000H microscope at two different magnifications. Electron micrographs were also recorded for SATEOS after dye adsorption at three different magnifications. Figs. 1a and 1b show the scanning electron micrographs of adsorbent before and after dye adsorption. SEM image of SATEOS (Fig.1b) showed that the pores were filled after the adsorption of MG dye on the SATEOS surface. Further SEM micrographs of SATEOS possess a rough surface morphology which can be taken as a sign for effective adsorption of MG molecules in the cavities of SATEOS surface. The presence of holes and cave type openings on the surface of the adsorbent indicate the availability of more surface area available for adsorption.[39]

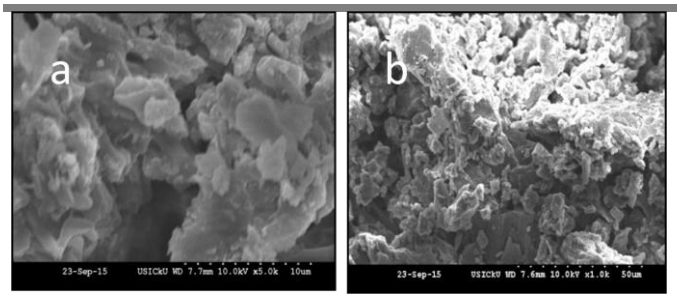

Fig.1(a): SEM pictures of sulphosalicylic acid doped tetraethoxysilane (SATEOS) before dye adsorption (a) 10μm and (b) 50μm magnifications

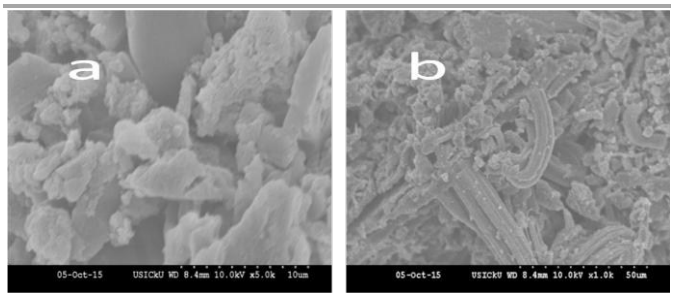

Fig.1(b): SEM pictures of sulphosalicylic acid doped tetraethoxysilane (SATEOS) after dye adsorption (a) 10μm (b) 50μm magnifications

3.2 Effect of contact time, initial dye concentration and adsorbent dose

Contact time significantly affected the dye uptake . The relation between MG removal and contact time were studied at various initial MG concentrations and adsorbent amounts, as contact time is known to depend on initial dye concentration and adsorbent dose.[40] The adsorption capacities for different doses were determined at definite time intervals by keeping all other factors constant. The percent adsorption enhances with the increase in SATEOS dose. For a constant initial MG concentration (30mL) removal percentage changes from 90.4-99.2% by changing adsorbent weight from 0.20-1.00g (Fig. 2(a) (Table S1)). The typical results of the dye removal percentage for different MG concentrations, is presented in Fig. 2(b) (Table S2). At each initial MG concentration, the increase in SATEOS dose enhances the MG diffusion. At higher SATEOS doses /concentration, there is a very fast superficial adsorption which can be attributed to increased SATEOS surface area and availability of more adsorption sites.[41] Rapid adsorption of dye occurs initially and equilibrium was achieved almost after 150 minutes of contact time, after that there is no sharp change in the adsorption process (Fig.3), increase in

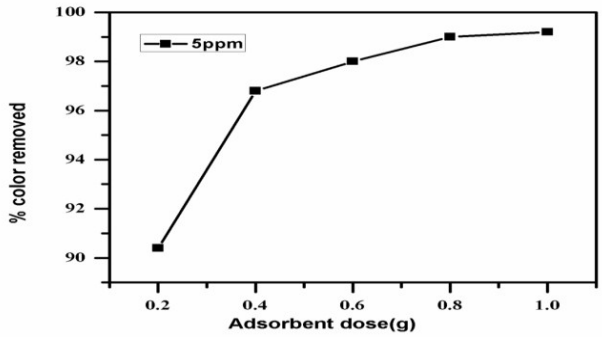

Fig. 2(a): Effect of SATEOS concentration on adsorption behaviour using 5ppm MG concentration

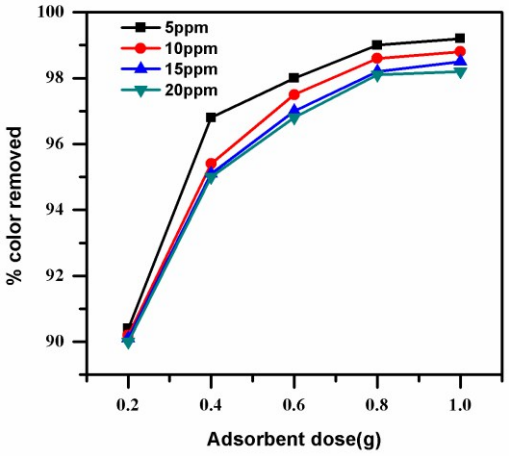

Fig. 2(b): Effect of SATEOS concentration on adsorption behavior using different MG concentrations

contact time after 180 minutes did not enhance the rate of adsorption. The progressive increase in adsorption and consequently, the attainment of equilibrium is initially due to the

presence of large number of active sites on the surface of SATEOS. After some time, number of available vacant sites goes on decreasing resulting in the decrease in adsorption rate. On account of repulsive forces between dye molecules on the SATEOS surface and the bulk phase, adsorption equilibrium was established.[42] The equilibrium data was collected and is summarized in Table S3. Time vs q_e plots obtained are smooth, single and continuous leading to saturation suggesting monolayer coverage of MG on the surface of SATEOS.[43] It could be said that higher the adsorbate concentration, the more diffusion would occur from the adsorbent surface into the micro pores. So, the initial rate of adsorption was greater for high initial MG concentrations and the resistance to the MG uptake diminished as the mass transfer driving force increased.

Adsorption behavior of SATEOS towards hazardous MG dye was carried out by passing aqueous solution of dye of varying concentrations (5ppm, 10ppm, 20 ppm) through SATEOS adsorbent column. In this experiment, a definite amount (250mL) of dye solution was passed through the column loaded with 1g of adsorbent material in H^+ form. Using UV-Visible spectrophotometer (Schimadz UV 3600), absorbance values were measured before and after passing the dye solutions through the column loaded with the adsorbent material and the result obtained is summarized in Table 1. From the data collected, it could be observed that with the increase in dye concentration from 5 to 20 ppm, the dye uptake increases from 4.7 ppm to 15.08 ppm. Absorbance pattern is shown in Fig. 4. This could be also due to the reason that the ratio of initial number of dye molecules to the number of available vacant sites on SATEOS surface are low at lower MG concentration but concentration gradient gets developed with the increase in initial dye concentration, which acts as a driving force to overcome mass transfer resistances of dye molecules leading to an increase in adsorption capacity till saturation is achieved.[23]

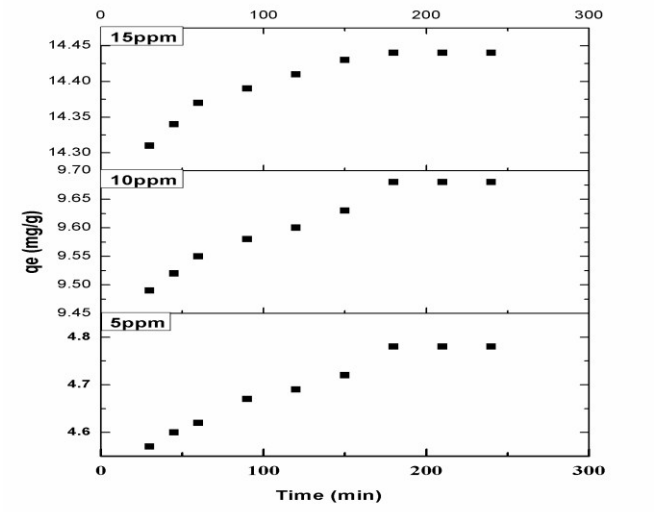

Fig.3: Effect of contact time on MG adsorption on SATEOS

Table 1 Effect of initial dye concentration on adsorption behavior of SATEOS

conc. before loading (ppm)	conc. after loading (ppm)	conc. difference (ppm)
5	0.3	4.7
10	1.30	8.7
20	4.92	15.08

3.3 Effect of pH

The pH of the aqueous solution of MG has significant effect on adsorption processes, particularly for adsorption capacity, as the removal of dyes from aqueous solution by adsorption is dependent on pH of the solution,[44] which affects the surface charge of the adsorbent, and degree of ionization of adsorbate (d molecule). Experiments were performed under the optimized conditions, which shows the effect of pH on MG removal by SATE (Fig. 5). As the solution pH increased, adsorption capacity of the SATEOS enhances, 94.02 % color removal efficiency was obtain at pH 9 and SATEOS concentration (0.2g) (Table 2) and beyond it, it did not change significantly. Being a basic dye, MG forms reduced ions (CNH^+) in solution, therefore extent of its adsorption on the SATEOS is influenced on the surface charge of SATEOS which in turn depends on solution pH. As the FTIR spectral analysis indicates, the presence of ionizable sulfonic functional groups (SO_3H^-) on surface which gets protonated at lower pH value thereby it does not allow positively charged dye cations to the surface of the SATEOS. At higher pH range, this group gets deprotonated and then adsorption process of MG proceeds because of electrostatic attraction between the negatively charged SATEOS surface and the positively charged dye cations.[44,28] Further, at lower pH value H^+ ions and dye cations compete for appropriate adsorption sites on the SATEOS surface, however this competition decreases at high pH values resulting in increased dye uptake on SATEOS surface. Interestingly, similar results have been reported earlier.[27,30]

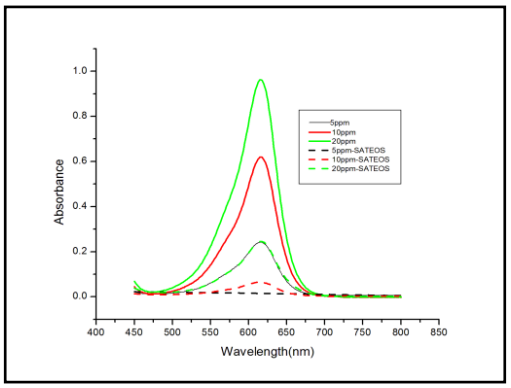

Fig. 4 : Effect of initial dye concentration on adsorption behaviour

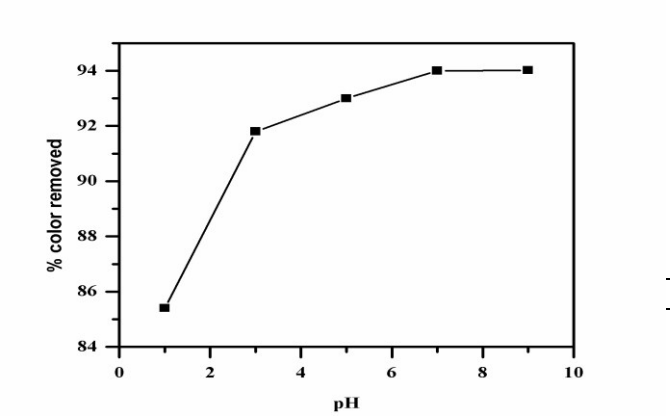

Fig. 5: Effect of pH on MG adsorption at 5ppm

3.4 Effect of temperature and thermodynamic Parameters

Adsorption experiments were carried out at different temperatures (30,40, and 50°C). Data collected from the experiments is presented in Table 3. The adsorption capacity of SATEOS increased with increase in the temperature of the system from 30°-50°C (Fig.6) indicating adsorption was kinetically controlled by an endothermic process.[28] It may be due to the reason that with the rise in temperature mobility and hence the kinetic energy of the molecules increases which enhanced the rate of adsorption.[45] The enhancement in the dye uptake capacity with increasing temperature can also be due to the higher affinity of adsorption sites for adsorbate molecules or due to the availability of more binding sites.[46]

Table 2 Effect of pH on MG adsorption conditions: (speed=120 rpm, wt. of adsorbent =0.2g, MG concentration =5ppm)

pH	% color removed
1	85.4
3	91.8
5	93.0
7	94.0
9	94.02

Thermodynamic parameters were evaluated using Van 't Hoff and Gibbs Helmholtz Eqs. (3)-(5).

$$K_c = \frac{C_0}{C_e} \qquad (3)$$

$$\Delta G^\circ = -RT\ln K_C \qquad (4)$$

$$\ln K_c = \left(\frac{\Delta S^\circ}{R}\right) - \frac{1}{T}\left(\frac{\Delta H^\circ}{R}\right) \qquad (5)$$

The Gibbs free energy change (ΔG°) indicates the feasibility of the adsorption process, while as ΔH° and ΔS° values indicate the change in enthalpy and spontaneity of the process respectively. Kc is the thermodynamic equilibrium constant. C_o and C_e are the initial and equilibrium concentration (mg/L) of dye in solution. Linear plot of ln K_c vs 1/T were obtained from which slope (ΔH°) and intercept (ΔS°) can be determined. The values of the thermodynamic parameters such as ΔH°, ΔS° and ΔG°, determined at 50 °C, are found to be 1.967 KJ/mol, 0.067 KJ/mol K and -10.251 KJ/mol, respectively. Endothermic nature of adsorption was confirmed by the positive value of ΔH°; whereas, feasibility and spontaneity of adsorption was confirmed by negative value of ΔG° and positive value of ΔS°, respectively. The reason for positive value of ΔS° can be due to overall gain in translational entropy as reported earlier.[47]

Table 3 Effect of temperature on MG adsorption conditions: (Wt. Of adsorbent = 0.2 g, volume solution = 25 mL, time period = 60 min)

Conc.(mg/L)	q_e (mg/g)		
	30°C	40°C	50°C
5	2.234	3.987	4.89
10	7.117	8.234	9.983
15	12.445	13.432	14.967

3.5 Adsorption isotherms

Adsorption isotherm expresses the relation between dye uptake per unit weight of adsorbent (q_e) and equilibrium concentration at a particular temperature. In order to investigate the maximum adsorption capacity of SATEOS for adsorption of MG, Two commonly used isotherm models, Langmuir and Freundlich, were applied to the experimental data in order to evaluate the applicability of the adsorption process.

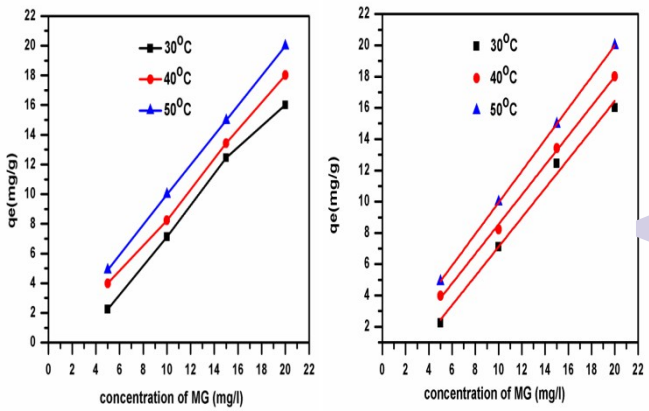

Fig. 6: Effect of temperature on MG adsorption

The Langmuir isotherm is valid for the monolayer adsorption process. It is expressed by the following equation.

$$\frac{1}{X/_m} = \frac{1}{\theta^\circ} + \frac{1}{\theta^\circ bC} \qquad (6)$$

Where θ° and b are Langmuir constants. θ° is related to adsorption capacity where as b is indicative of adsorption energy . X/m is the dye uptake per unit weight of adsorbent (mg/g) and C is the concentration of dye (mg/L). Langmuir constant (θ° and b) are obtained from the intercept and slope of the linear plots[48,49] of 1/X/m vs 1/C (Table S4) (Fig. 7).

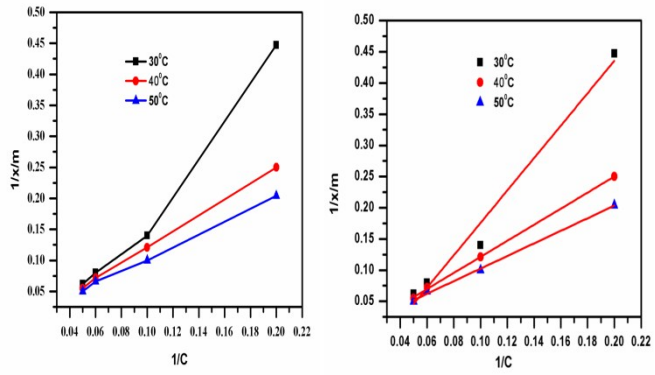

Fig. 7: Langmuir isotherm model for MG adsorption

As can be seen from Table 4, the Langmuir isotherm model showed excellent fit to the experimental data with high correlation coefficients particularly at high temperatures, as MG adsorption on SATEOS was affected by temperature. In addition, θ° increases with increasing temperature indicating temperature induced a higher maximum adsorption capacity. The monolayer adsorption capacity of SATEOS for MG as obtained from the Langmuir isotherm at 323K was found to be 657.89 mg/g (Table 4).

Dimensionless separation factor R_L which is expressed as;

$$R_L = {}^{1}/_{1 + bC_0} \qquad (7)$$

depicts whether the adsorption is favourable or unfavorable. C_0 is the initial dye concentration (mg/L) and b is the Langmuir constant (1/mg). It indicates the shape of the isotherm to be either unfavorable (R_L >1), linear (R_L = 1) , irreversible (R_L = 0) or favourable (0 < R_L < 1). Our experimental results show that the value of R_L ranges between 0 and 1 indicating favourable adsorption.[50,51]

The linear Freundlich equation is expressed by the following equation.

$$log\frac{X}{m} = logK_f + \left[\frac{1}{n}\right] log \qquad (8)$$

K_f and n are Freundlich constants. K_f indicates adsorption capacity, while as n is indicative of adsorption intensity of dye on the adsorbent surface (surface heterogeneity) which in turn is a cooperative adsorption).[48,49] The Freundlich model also showed a good fit to the experimental equilibrium data at all temperatures studied (R^2 > 0.98) (see Table 4). Applicability of this model was assessed by plotting log x/m vs log C (Table S5) (Fig. 8). The adsorption capacity, K_f decreases with increasing temperature indicating adsorption capacity was governed by temperatu Further larger values of n suggest strong interaction between the adsorbent and the dye molecules.[52] From the above discussion it could be concluded that both the isotherms can explain the adsorption process with Langmuir having high applicability.

Table 4 Isotherm constants of MG adsorption onto SATEOS

Isotherm	Equation	Parameters	Temperature(°C)		
			30	40	50
Langmuir	1/ x/m =1 / θ° + 1 /θ° bC	θ° (mg/g)	11.904	135.135	657.894
		b(1/mg)	0.03	0.005	0.001
		R_L	0.862	0.975	0.995
		R^2	0.973	0.999	0.997
		qe (cal)			
		5ppm	2.237	4	4.901
		10ppm	7.142	8.264	10
		15ppm	12.5	13.888	15.151
		20ppm	16.129	18.181	20
Freundlich	logx/m=logK_f+[1/n]logC	K_f [(mg/g) (mg/l)$^{1/n}$]	4.305	1.472	1.039
		n	0.692	0.914	0.987
		R^2	0.982	0.998	0.999
		qe (cal)			
		5ppm	2.233	3.981	4.886
		10ppm	7.122	8.222	9.977
		15ppm	12.445	13.427	14.962
		20ppm	15.995	17.988	19.952
Experimental data		**qe (cal)**			
		5ppm	2.234	3.987	4.89
		10ppm	7.117	8.234	9.983
		15ppm	12.445	13.432	14.967
		20ppm	16.002	18.01	19.989

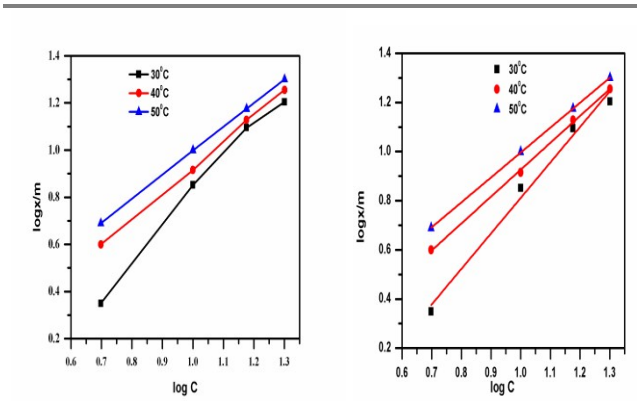

Fig. 8 : Freundlich isotherm model for MG adsorption

3.6 Adsorption kinetics

The kinetics of dye removal was carried out to understand the adsorption behaviour of SATEOS. Two different kinetic models have been used to investigate the adsorption kinetics, like Lagergren first order kinetic model (Eqn. (9))[50] and pseudo second order kinetic model (Eqn. (10)).[51,53]

$$log(q_e - q) = log q_e - K_1 \frac{t}{2.303} \qquad (9)$$

$$t\left(\frac{1}{q_t}\right) = t\left(\frac{1}{q_e}\right) + \frac{1}{K_2} qe^2 \qquad (10)$$

Where q_t and q_e represent the amount of dye adsorbed (mg/g) at any time and at equilibrium time respectively, K_1 represents first order rate constant (min^{-1}) while as K_2 is the pseudo second order rate constant (g mg^{-1} min^{-1}). The experimental results were modeled to above mentioned kinetic models and the values of their estimated parameters are shown in Table 5. The graph of the log (q_e -q_t) vs time (Table S6) (Fig.9) exhibits straight lines at lower concentrations but shows deviation at higher concentration. The conformity between experimental data and the values predicted by any model is expressed by R^2 values. Good and reasonable fits were obtained at lower concentrations which significantly deteriorates at higher concentrations indicating Lagergren first order kinetic model cannot be completely applicable to our system. The graph of t/q_t vs time (Table S7) (Fig.10) exhibits straight lines for different concentrations and do not show deviation at higher concentrations confirming pseudo second -order rate kinetics for the on-going adsorption process. q_e and k_2 values were determined from the slope and intercept of plots. The correlation coefficients, obtained from pseudo second order kinetic model, are close to 1 in the first two cases and equal to 1 for 15ppm (Table 5). Moreover, it can be seen from the Table 5 that the calculated values of qe were close to the experimental uptake value showing applicability of this model for evaluating and fitting experimental data over entire adsorption process[54] and, therefore, it supports the assumption of the model that chemisorptions may be one of the modes of adsorption.

Table 5 Kinetic parameters of MG adsorption onto SATEOS

Models	Equation	Parameters	Concentration (ppm)		
			5	10	15
First order kinetic model	$log(q_e-q) = logq_e - K_1t/2.303$	K_1	0.0102	0.0105	0.0197
		qe(cal)	0.288	0.257	0.250
		R^2	0.991	0.983	0.951
Second order kinetic model	$t(1/q_t) = t(1/q_e) + 1/K_2qe^2$	K_2	0.092	0.111	0.228
		qe(cal)	4.81	9.705	14.465
		R^2	0.999	0.999	1
Reichenberg equuation	$B_t=[-2.303\ log(1-F)](0.4997)$	B_t	0.01	0.009	0.016
	$F = Q_t / Q_0$	D_i	$1.04x10^{-3}$	$9.128x10^{-4}$	$1.622x10^{-3}$
	$B_t = [\pi^2 D_i]/r_0$	R^2	0.994	0.99	0.911
Experimental data		**qe(exp)**	4.57	9.49	14.31

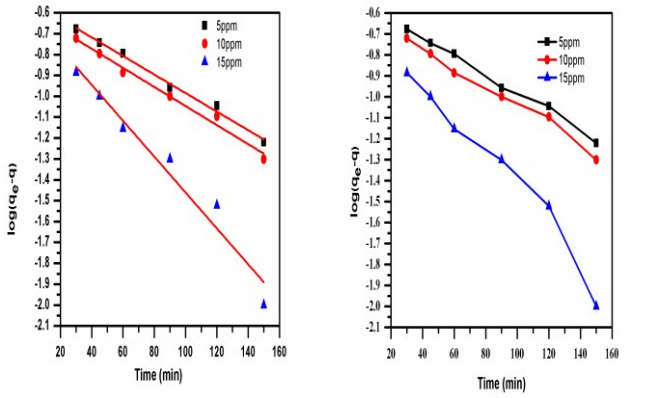

Fig. 9: Lagergren first order kinetic model

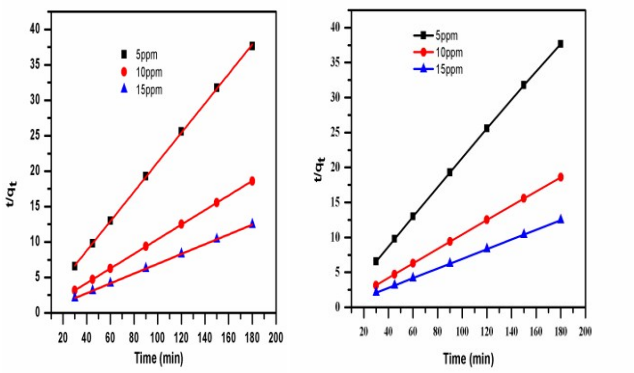

Fig. 10: Pseudo second order kinetic model

Kinetic data were analysed using Reichenberg Eqs. (11)- (13)[55]

$$B_t = [-2.303\log(1-F)] - (0.4997) \qquad (11)$$

$$F = \frac{Q_t}{Q_0} \qquad (12)$$

$$B_t = \left[\frac{\pi^2 D_i}{r_0}\right] \qquad (13)$$

Where,

F = Fractional attainment of equilibrium at time t

Q_t = Amount of adsorbate taken up at time t

Q_0 = Maximum equilibrium uptake at infinite time

D_i = Effective diffusion coefficient of adsorbate in the adsorbent phase

B_t = Time constant

r_o = Radius of the adsorbent particle assumed to be spherical

Adsorption process of an adsorbate (organic/inorganic) over an adsorbent involves the following main steps:

(i) Film diffusion (internal transport > external transport)

(ii) Particle diffusion (external transport > internal transport)

Kinetic experiments were performed at three different concentrations (5ppm, 10ppm, 15ppm) and the data collected can be seen in Table 5 and Table S8 where linearity test of Bt versus time plots were used to explain the adsorption mechanism. It has been reported that particle diffusion mechanism is active if plot of Bt against time is linear and has zero intercept, however adsorption is governed by film diffusion for a linear or non linear relationship with intercept value different than zero.[56,57] In this study, plots for all the concentrations of MG are almost linear (Fig.11) but are not passing through the origin, and at higher concentration plots obtained show deviations from linearity confirming film diffusion controlled adsorption mechanism. The straight lines obtained from the graph of log (1-F) vs time (Fig.12) for different MG concentrations are also helpful in determining the fact that adsorption occurs via internal transport again confirming film diffusion.[28]Adsorption behavior is influenced by many factors such as adsorbent surface properties, steric effect and hydrogen bonding, Vander Waals forces, etc. In our experiment we observed that adsorption behavior was highly dependent on pH. With the increase in pH, rate of adsorption increases indicating adsorption occurs through the chemisorption.[55] The possibility of physisorption cannot be ruled out as good correlation coefficients were obtained from Freundlich adsorption isotherm indicating possibility of multilayer adsorption.

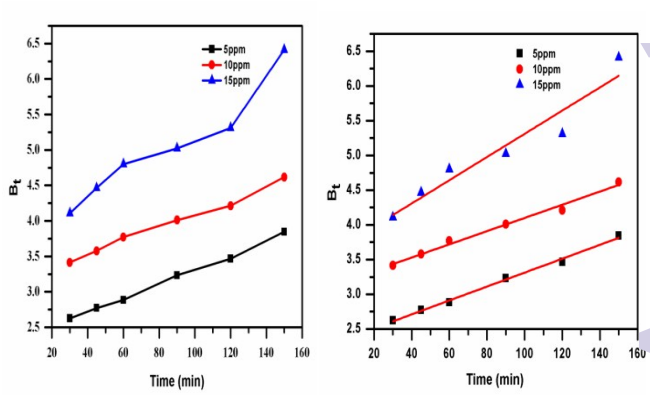

Fig. 11: Bt Vs time plot for MG adsorption

3.7 Desorption studies

Finally desorption studies were carried out which enables the recovery of the dyes from waste water and regeneration of the adsorbent which is economically effective. Using water of neutral pH for desorption of the adsorbed dye indicates that the attachment of the dye with the adsorbent is by weak bonds. Use of sulphuric acid or alkaline water for the same process indicates that the adsorption is by ion exchange. However, if organic acids like acetic acid can desorb the dye, then the dye holds the adsorbent through chemisorptions.[58] In our experiment, desorption was studied by column process using 1 g of SATEOS in H^+ form. 0.1M and 1M CH_3COOH are used as eluents for the regeneration of exhausted columns at the flow rate of 1ml/min confirming chemisorption. It was used to desorb MG solution of concentration (15 ppm).UV-Visible spectrophotometer (Schimadzu UV 3600) was used to determine the equilibrium concentration of MG. The MG loaded adsorbent was washed with deionized water several times. Increase in concentration of acetic acid enhances the percentage of desorption. Complete desorption of MG could not be achieved confirming chemisorption as the mode of adsorption.[55]

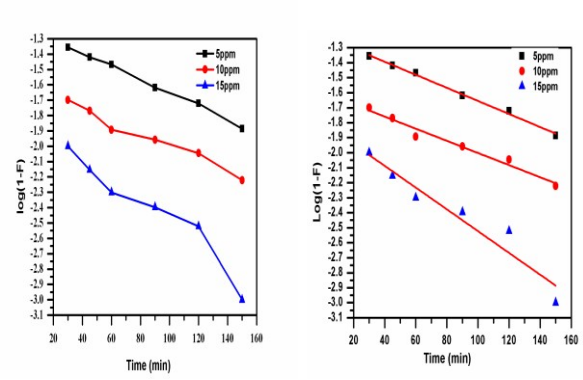

Fig. 12 : Plot of Log (1 - F) vs time for MG adsorption on SATEOS

3.8 Computational details

We performed quantum mechanical computations on the dye, SATEOS and their combination (SATEOS-dye) model systems in order to simulate IR spectra using density functional theory to know the possible interaction between the dye and SATEOS molecules. The optimized geometries of SATEOS, dye and model system (SATEOS-dye) are shown in Fig. 13. From the spectra (Fig.14), it is clear that in combination (SATEOS-dye), the peaks corresponding to OH stretching (3600-4000 cm^{-1}) shifts towards the lower wave number and peak intensity diminish as compared to dye or SATEOS reflecting a possible interaction between the nitrogen of dye with that of the hydrogen atom present on hydroxyl group. The interaction energy was calculated using the following equation.

$$\Delta E = E_{SATEOS+dye} - \left[E_{SATEOS} + E_{dye}\right] \qquad (14)$$

The maximum interaction was observed between SATEOS and dye molecule with an interaction energy of 1432.54 KJ $(mole)^{-1}$, when the nitrogen atom of dye lies at a distance of 1.57Å from the hydrogen of hydroxyl group present on SATEOS molecule.

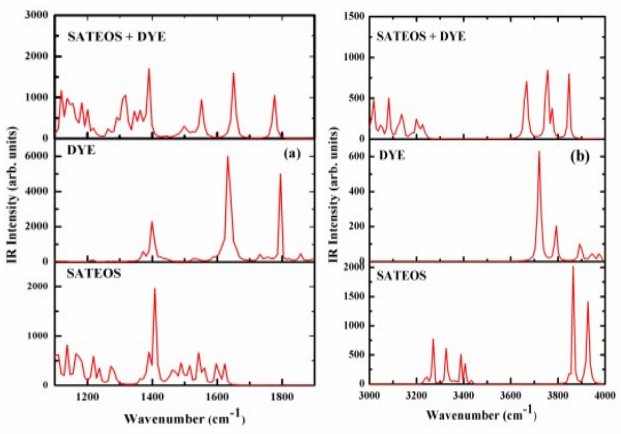

Fig. 13 : Simulated IR spectra of SATEOS- dye combination in the region (a) 1200– 1800 cm^{-1} and (b) 3000–4000 cm^{-} calculated by employing (B3PW91) and LanL2MB basis set

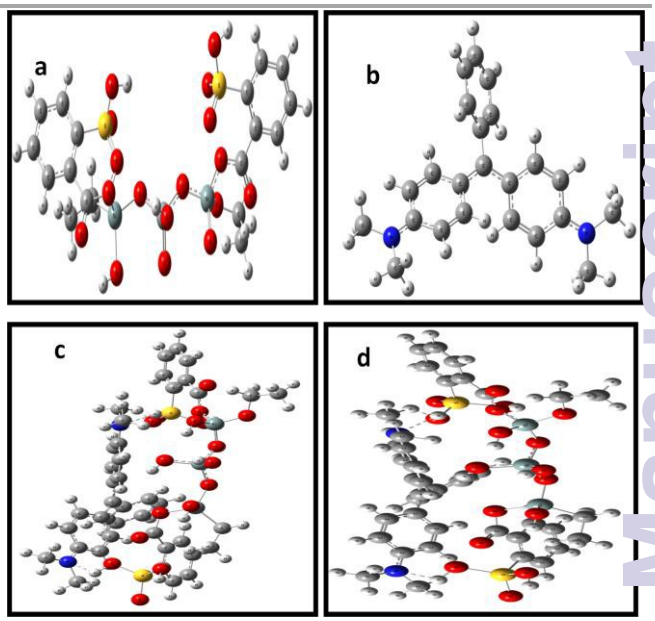

Fig. 14: Optimized geometries of (a) SATEOS (b) dye (c) SATEOS- dye combination (view 1) (d) SATEOS-dye combination (view 2) calculated by employing (B3PW91) and LanL2MB basis set

4. Conclusions

The research work illustrates the use of SATEOS composite material as an effective adsorbent for the removal of MG from aqueous solutions. The maximum monolayer adsorption capacity of SATEOS was found to be 657.89 mg/g at 323 K. The adsorption kinetics follows the pseudo-second-order kinetic model and the adsorption was controlled by film diffusion mechanism. The adsorption process was spontaneous and endothermic in nature. The experimental data correlated reasonably well with the Langmuir and Freundlich adsorption isotherms and the respective isotherm parameters were calculated. The dimensionless separation factor also shows that the SATEOS can be used for the removal of MG from aqueous solution.

Acknowledgements

We are thankful to the Head, Department of Chemistry, University of Kashmir, for providing the necessary laboratory facility for carrying out this work. A.H.P. thanks the University Grants Commission (UGC), Government of India for research grant [F.No.42-305/2013(SR)].

References

1 M. A. Al-Ghouti, M. A. M. Khraisheh, S. J. Allen and M. N. Ahmad, *J. Environ. Manage.,* 2003, **69**, 229.
2 O. Hamdaoui, *J. Hazard. Mater.,* 2006, **38 (2)**, 293–303.
3 X. S. Wang, Y. Zhou, Y. Jiang and C. Sun, *J. Hazard.Mater.* 2008, **157 (2–3)**, 374–385.
4 E. Bulut, M. Ozacar and I. A. Sengil, *Micropor. Mesopor. Mater.,* 2008, **115 (3)**, 234–246.
5 J. Zhang, Y. Li, C. Zhang and Y. Jing , *J. Hazard. Mater.* 2008, **150**, 774–782.
6 M. Rafatullah, O. Sulaiman, R. Hashim and A. Ahmad , *J.Hazard. Mater*., 2010,**177**, 70–80.

7 K. Y. Foo and B. H. Hameed, *Chem. Eng. J.,* 2010, **156**, 2–10.
8 C. Kannan, T. Sundaram and T. Palvannan, *J. Hazard. Mater.,* 2008, **157**, 137.
9 P. Tzvetkova, P. Vassileva and R. Nickolov, *J. Porous. Mater.,* 2010, **17**, 459.
10 N. Kawasaki, F. Ogata and H. Tominaga, *J. Hazard. Mater.,* 2010, **181**, 574.
11 K. Hamada, T. Kaneko, M. Q. Chen and M. Akashi, *Chem. Mater.,* 2007, **19**, 1044.
12 W. S. Wan Ngaha, L. C. Teong and M. A. K. M. Hanafiah, *Carbohydrate Polymers,*2011, **83**, 1446–1456.
13 J. G. Yu , L. Y. Yu, H. Yang, Q. Liu, X. H. Chen, X. Y. Jiang, X. Q. Chen and F. P. Jiao, *Sci. Total Environ.,* 2015, **502**, 70- 79.
14 J. G. Yu, X. H. Zhao, H. Yang, X. H. Chen, Q. Yang, L. Y. Yu, J. H. Jiang and X. Q. Chen, *Sci. Total Environ.,* 2014, **482–483,** 241–251.
15 V. Rocher, J-M. Siaugue, V. Cabuil and A. Bee, Water Res., 2008, **42**, 1290–1298.
16 L. Wang, and A. Wang, J. Hazard. Mater., 2007, **147**, 979–985.
17 R. Gong, Y. Jin, F. Chen, J. Chen and Z. Liu, *J. Hazard. Mater.,*2006, **137(2)**,865–870.
18 S. Srivastava, R. Sinha and D. Roy, *Aquat. Toxicol*, 2004, **66 (3)**, 319.
19 J. Chen, J. Mao, X. Mo, J. Hang and M. Yang, *Coll. Surf., A.* 2009, **345 (1– 3)**, 231–236.
20 V. K. Gupta and Suhas, *J. Environ. Manage.,* 2009, **90**, 2313–2342.
21 A. Mittal, *J. Hazard.Mater.B*, 2006, **133**, 196–202.
22 K. G. Bhattacharyya, *Dyes. Pigments,* 2003, **57**, 211–222.
23 S. Chowdhury, R. Mishra, P. Saha and P. Kushwaha, *Desalination,* 2011 **265**, 159–168.
24 K. V. Kumar, *Dyes. Pigments,* 2007, **74**, 595–597.
25 B. H Hameed and M. I. El-Khaiary, *J. Hazard. Mater.,* 2008, **159**, 574–579.
26 P. Saha, S. Chowdhury, S. Gupta, I. Kumar, and R. Kumar, *Clean: Soil Air Water,* 2010, **38**, 437–445.
27 M –H. Baek, C. O. Ijagbemi, O. Se-Jin and D-S . Kim, *J. Hazard. Mater.,* 2010, **176**, 820–828.
28 R. Ahmad and R. Kumar, *J. Environ. Manage.,* 2010, **91**, 1032–1038.
29 A. Mendez, F. Ferna´ndez and G. Gasco, *Desalination,* 2007, **206**, 147–153.
30 B. H Hameed and M. I. El-Khaiary, *J. Hazard. Mater.,* 2008, **157**, 344–351.
31 T. Santhi, S. Manonmani and T. Smitha, *J. Hazard. Mater.,* 2010, **179**, 178–186.
32 S. D. Khattria and M. K. Singh, *J. Hazard. Mater*., 2009, **167**, 1089–1094.
33 P. Saha, S. Chowdhury and S. Gupta, I. Kumar, *J . Chem. Eng.,* 2010, **165**, 874–882.
34 A. S. Franca, L. S. Oliveira, S. A. Saldanha, P. I. A. Santos and S. S. Salum, *Desalin. Water Treat*., 2010, **19**, 241–248.
35 S. Rehman, N. Islam, S. Ahad, S. Z. Fatima and A.H. Pandith, *J.Hazard. Mater*.,2013, **260**, 313– 322.
36 M. J. Frisch, G. W. Trucks, H. B. Schlegel, G. E. Scuseria, M A. Robb, J. R. Cheeseman, J. A. Montgomery Jr., T. Vreven, K. N. Kudin, J. C. Burant, J. M. Millam, S. S. Iyengar, J. Tomasi, V. Barone, B. Mennucci, M. Cossi, G. Scalmani, N. Rega, G.A. Petersson, H. Nakatsuji, M. Hada M. Ehara, K. Toyota, R. Fukuda, J. Hasegawa, M. Ishida, T.Nakajima, Y. Honda, O. Kitao, H. Nakai, M. Klene, X. Li, J.E. Knox, H.P. Hratchian, J.B. Cross, V. Bakken, C. Adamo, J. Jaramillo, R. Gomperts, R. E. Stratmann, O Yazyev, A. J. Austin, R. Cammi, C. Pomelli, J. W. Ochterski, P. Y. Ayala, K. Morokuma, G. A. Voth, P Salvador, J. J. Dannenberg, V. G. Zakrzewski, S. Dapprich, A. D. Daniels, M. C. Strain, O. Farkas, D. K. Malick, A. D Rabuck, K. Raghavachari, J. B. Foresman, J. V. Ortiz, Q. Cui, A. G. Baboul, S. Clifford, J. Cioslowski, B. B. Stefanov, G. Liu, A. Liashenko, P. Piskorz, I. Komaromi, R. L. Martin, D. J. Fox, T. Keith, M. A. Al-Laham, C. Y Peng, A. Nanayakkara, M. Challacombe, P. M. W. Gill, B Johnson, W. Chen, M. W. Wong, C. Gonzalez and J. A Pople, *GAUSSIAN 03 Revision B.03, Gaussian, Inc, Wallingford, CT,* 2004.
37 J. P. Perdew, J. A. Chevary, S. H. Vosko, K. A. Jackson, M. R. Pederson and D. J. Singh, *Phys. Rev. B.,* 1992, **4**, 6671- 6687.
38 (a) W. J. Hehre, R. F. Stewart and J. A .Pople , *J. Che Phys.,* 1969, **51**, 2657.
(b) J .B. Collins, P. V. R. Schleyer, J .S . Binkley and J. A . Pople, *J. Chem. Phys.,*1979, **64**, 5142.
39 S. D. Khattri and M. K. Singh, *Ind .J. Chem. Tech* 1999, **6**, 112.
40 M. Ghaedi, M. Nejati Biyareh, S. Nasiri Kokhdan, S. H. Shamsaldini, R. Sahraei, A. Daneshfar and S. Shahriyar, *Mater. Sci. Eng.,* 2012, **C 32 (4)**, 725.
41 N. Nasuha, B. H. Hameed and A. T. M. Din, *J. Hazard.Mater.,* 2010, **175**, 126–132.
42 I. D. Mall, V. C. Srivastava and N. K. Agarwal, *J. Hazard. Mater.,* 2007, **143**, 386–395.
43 A. Bhatnagar, A. K. Minocha, and M. Sillanpaa, *J. Biochem. Eng.,* 2010, **48**, 181–186.
44 S. Chowdhury and P. Das (Saha), *Separation Science and Technology,* 2011, **46**, 1966–1976.
45 K. G. Varshney and A. H. Pandith, *Langmuir,* 1999, **15** 7422-7425.
46 S. Kiran, N. Ilhan, C. Caner, F. Iscen and Z. Yildiz, *Desalination,* 2009, **249**, 273–278.
47 Y. Zhou, M. Zhang, X. Wang, Q .Huang, Y. Min, T. Ma and J. Niu, *Ind. Eng. Chem. Res*., 2014, **53**, 5498−5506.
48 D. G. Krishna and G. Bhattacharyya, *Appl. Clay Sci.* 2002, **20**, 295.
49 S. Arivoli, M. V. Jain and T. Rajachandrasekar, *Mat. Sci. Res*., 2006, **3**, 241-250.
50 K. Periasamy, and C. Namasvayam, *Indus. Eng. Chem. Res.,* 1994, **33**, 317–320.
51 Y. S Ho and G. Mckay, *Dept. Chem. Eng.,* 1998, **7**, 313–318.
52 S. Chowdhury and P. Das , *Dept. Biotech.,* 2012, **31**, 415-425.
53 Y. S. HO , *Water.res.,* 2005, **40**, 119-125.
54 M. Ghaedi, B. Sadeghian, A. Amiri Pebdani, R. Sahraei, A. Daneshfar and C. Duran, *J. Chem. Eng.,* 2012, **18**, 133.
55 D. Reichenberg, *J. Am. Chem. Soc.,* 1953, **100**, 75: 589–597.
56 A. Mittal, *J. Hazard. Mater.,* 2006, **133**, 196–202.

57 A. A. Khan and S. Shaheen , *J. Indus. and Eng. Chem.,* doi:10.1016/j.jiec.2014.11.028.

58 B. R. Venkatraman, K. Hema, V. Nandhakumar and S. Arivoli, *J. Chem. Pharm. Res.,* 2011, **3(2)**, 637-649.